Supplementary Data

Asymmetric cell division requires specific mechanisms for adjusting global transcription

Adriana Mena; Daniel A. Medina; José García-Martínez; Victoria Begley; Abhyudai Singh; Sebastián Chávez; Mari C. Muñoz-Centeno and José E. Pérez-Ortín

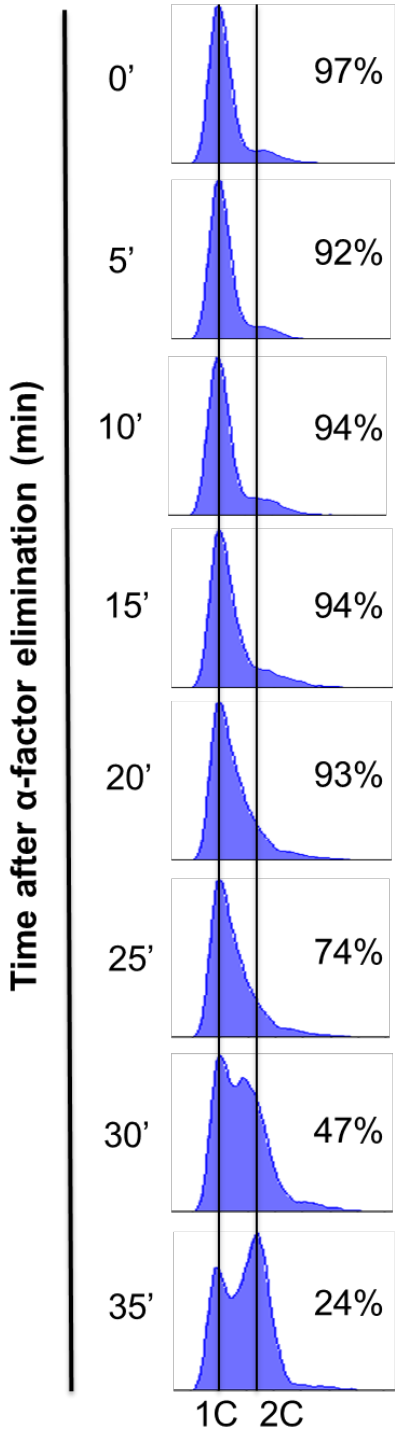

Figure S1. Cytometry study of the experiment described in Figures 2C-D and 3. The wild-type (BY4741) cells grown asynchronously were synchronized at START by a treatment with α-factor for 2 hours at 30°C (time 0). Cells were then released from the arrest at time 0 by washing out the α-factor. Samples were taken at different time points to analyze DNA content by flow cytometry and the proportion of unbudded cells by optical microscopy. The percentage of unbudded cells at each point is indicated. Other samples were taken at the same time points to perform the estimations represented in Figure 3.

A)

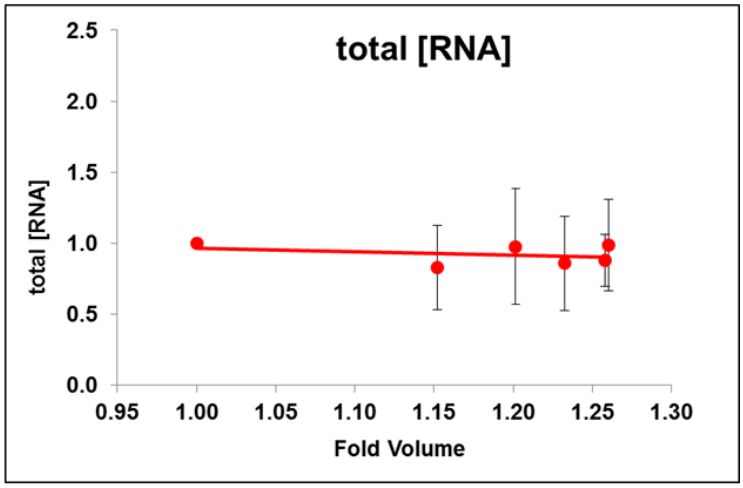

B)

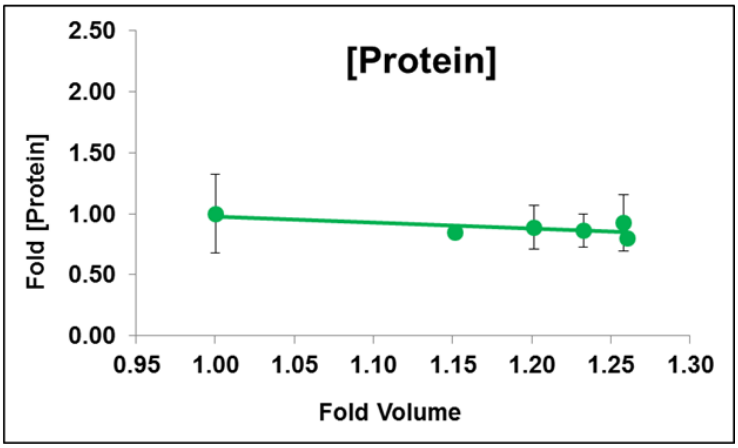

C)

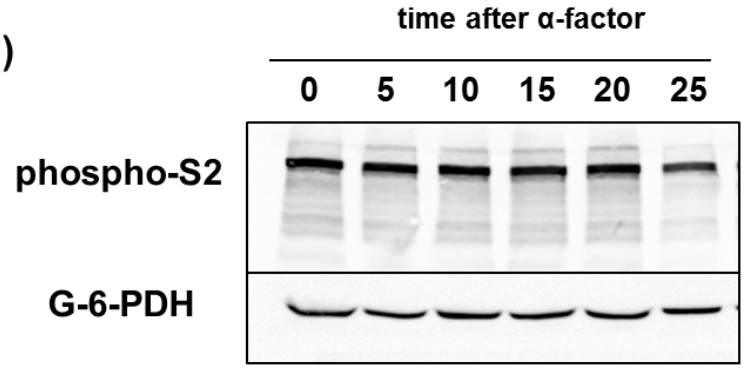

Figure S2. Ribostasis and proteostasis analysis in synchronized cells. A) The total RNA concentration in yeast cells regarding cell volume. B) Total protein determined by the Bradford protocol from aliquots of the same samples. C) An example of the Western blot used for Figure 3C. The RNA pol II levels were normalized against the internal control of Pgk1p. This figure is complementary to Figure 3.

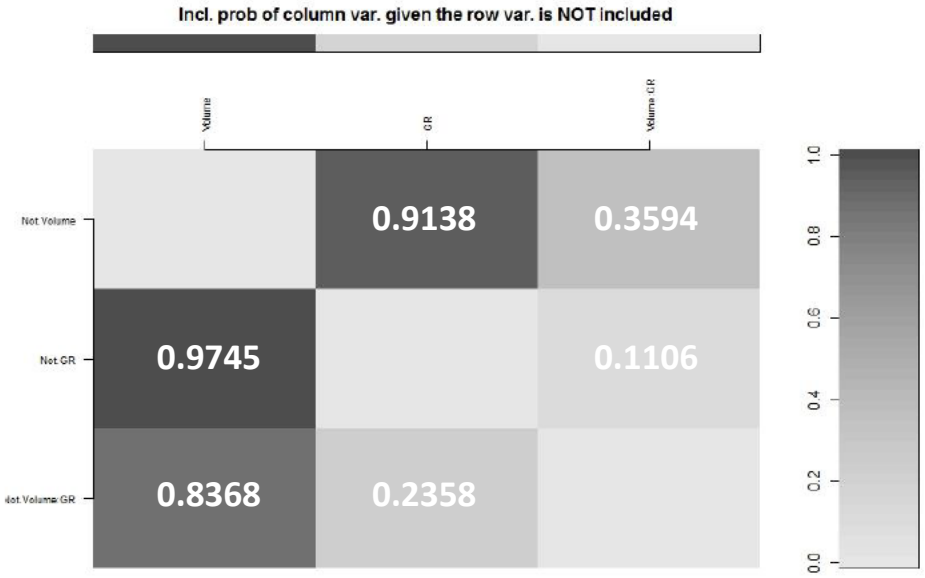

Figure S3. Statistical test for the determination of the cross-dependence of cell volume, growth rate (GR) and mRNA synthesis rates (SRII). A Bayesian probabilistic analysis to test the interdependence of GR and the cellular volume in relation to SRII was done. The numbers in the figure reflect the inclusion probabilities of the variables in columns if the variables in rows are not included. With this model, we conclude that volume and SRII are related and that just one of them should be included in the model, preferably volume, and not GR. This conclusion is supported by a conditional posterior probability of 0.83 of including volume when GR is excluded. Related to Figure 4.

A)

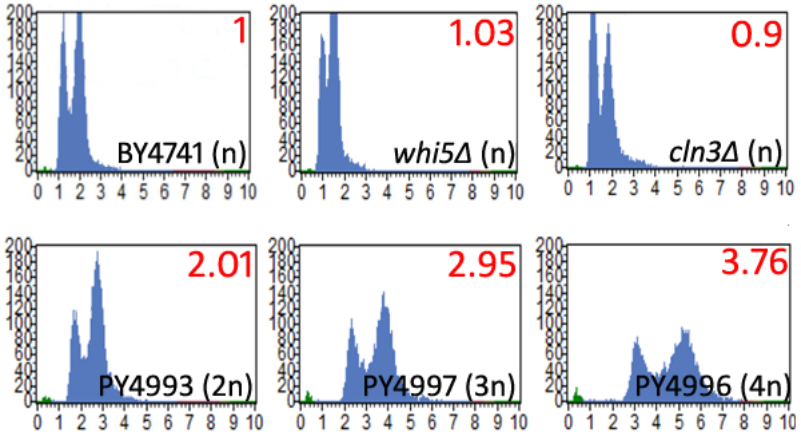

B)

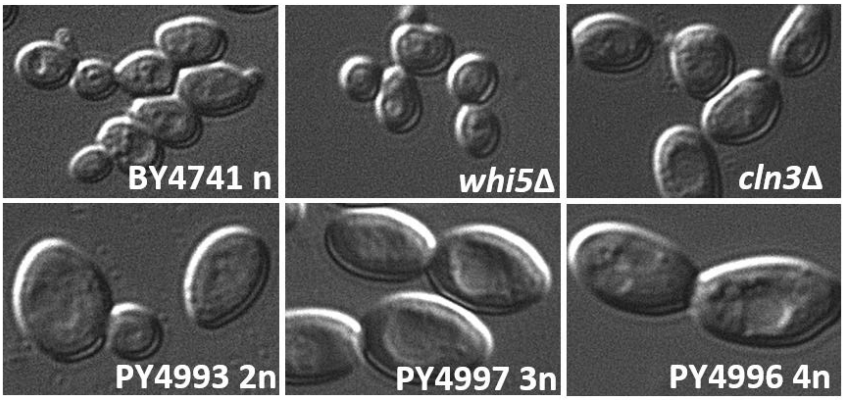

C)

Strain	Genome features	Ploidy	Doubling time (hrs)	Volume (fL)	Relative Volume	Relative DNA content	Relative total [mRNA] dotblot measure	Relative total [mRNA] flow cytometry measure	Relative total [RNA]
BY4741	wt	n	1.7	50 ± 4.3	1	1	1.00	1.00	1.00
BQS2006	*cln3Δ*	n	1.9	83 ± 9.9	1.68	0.9	0.82	0.83	0.73
JCY0704	*whi5Δ*	n	1.9	38 ± 2.5	0.76	1.03	0.77	1.03	1.00
PY4993	wt	2n	1.7	78 ± 4.9	1.57	2.01	0.67	1.22	1.23
PY4997	wt	3n	1.7	112 ± 7.9	2.26	2.95	0.94	0.98	0.86
PY4996	wt	4n	1.7	140 ± 9.7	2.83	3.76	1.28	0.96	0.83

Figure S4. Biological data for the polyploid and cell size mutant strains. A) The cytometry analysis of the six strains used in the experiments shown in Figures 5 and 6. B) Phase contrast micrographies of the same strains. C) Table showing all the biological relevant data from these strains used throughout the present study.

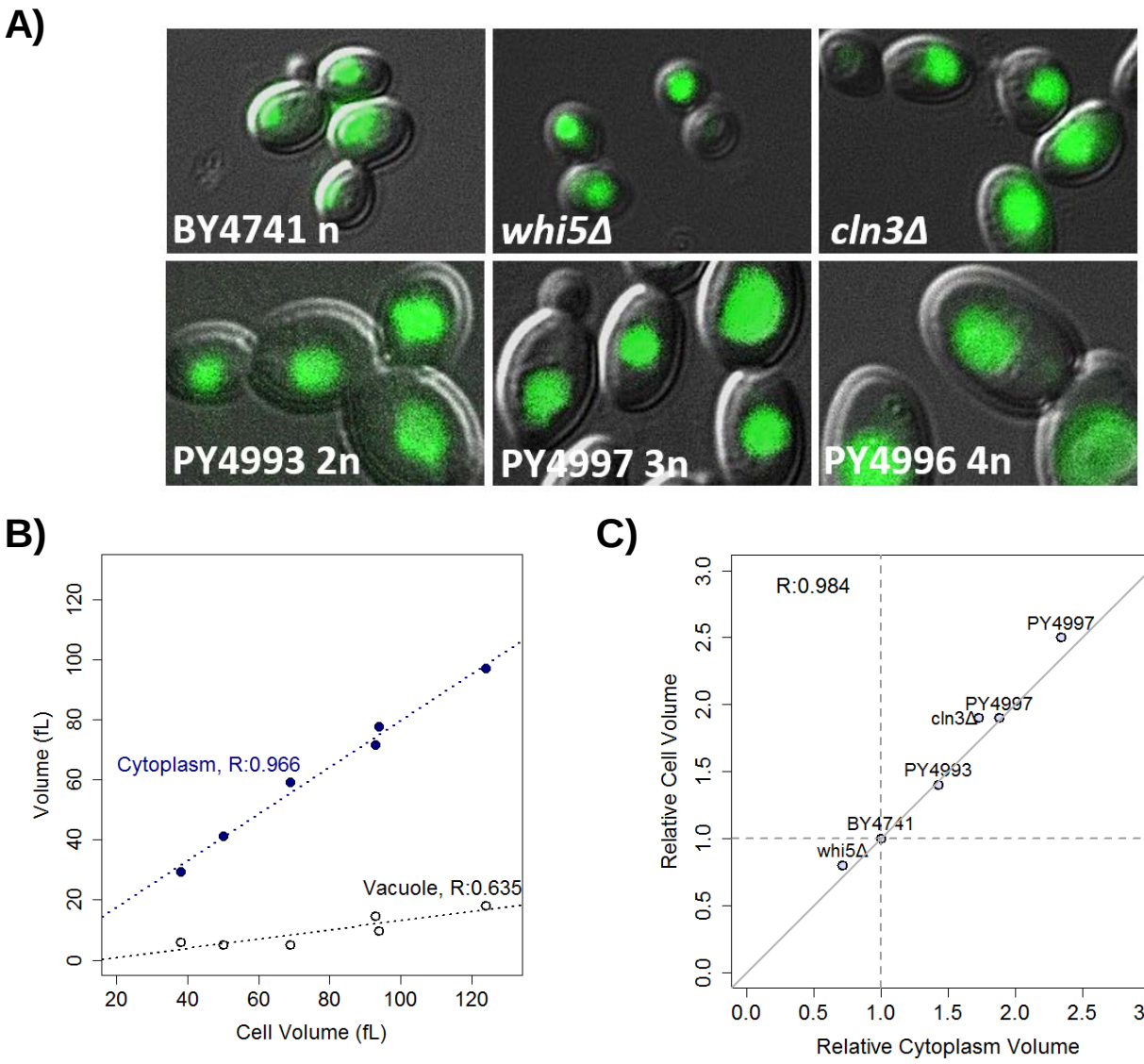

Figure S5. Study of the influence of vacuole size on the measured cytoplasmic volumes. It is known that vacuole size is strain-dependent and that it also increases slightly faster than the total cell volume (Chan and Marshall, 2014). However, we found that if we corrected the data in Figure S3 by the vacuole size effect, the proportion of cell size between the different strains showed almost no change. It is noteworthy, however, that our volume calculations made by a Coulter-Counter device (median value of >30,000 cell population) gave a different value from that obtained by the original authors by microscope imaging of 100 cells (Storchova et al., 2006). We found that volume increased less than the average DNA amount per cell (see Supplementary Figure S4C), unlike that found by them. We do not know the reason for such discrepancy, but we are confident with our results because the increase in volume and ploidy, by microscope imaging, in another genetic background was not shown to be proportional (Galitski et al., 1999). Related to Figures 5 and 6.

Supplementary references

-Chan, Y.H. and Marshall, W.F. (2014). Organelle size scaling of the budding yeast vacuole is tuned by membrane trafficking rates. Biophys J. 106, 1986-1996.

-Galitski, T., Saldanha, A.J. Styles, C.A., Lander, E.S. and Fink, G.R. (1999). Ploidy regulation of gene expression. Science 285, 251-254.

Genes decreasing slower in SR	Description	P-value
GO:0032196	transposition	1.07E-06
GO:0022900	electron transport chain	4.44E-06
GO:0006091	generation of precursor metabolites and energy	5.49E-05
GO:0015986	ATP synthesis coupled proton transport	2.57E-04
GO:0070469	respiratory chain	2.57E-04
Genes decreasing faster in SR	**Description**	**P-value**
GO:0005886	plasma membrane	7.14E-06
GO:0019236	response to pheromone	1.84E-06
GO:0000025	maltose catabolic process	4.55E-04
GO:0051321	meiotic cell cycle	6.84E-04

Figure S6. Analysis of the gene functional groups with differential behaviors as regards the average population. The genome-wide experimental data set used for the global SRII calculation was used to calculate individual gene profiles as regards cell volume. This genomic gene set was ordered by the slope values of the linear regression lines. This ordered set was analyzed by a gene set enrichment analysis to find Gene Ontology (GO) functional categories that were significantly biased toward the top of the ordered list (genes decreasing more slowly than the average) or to the bottom of the list (genes decreasing more quickly than the average). Note that the average population SRII displays a decreasing behavior (Figure 5A, blue dots).

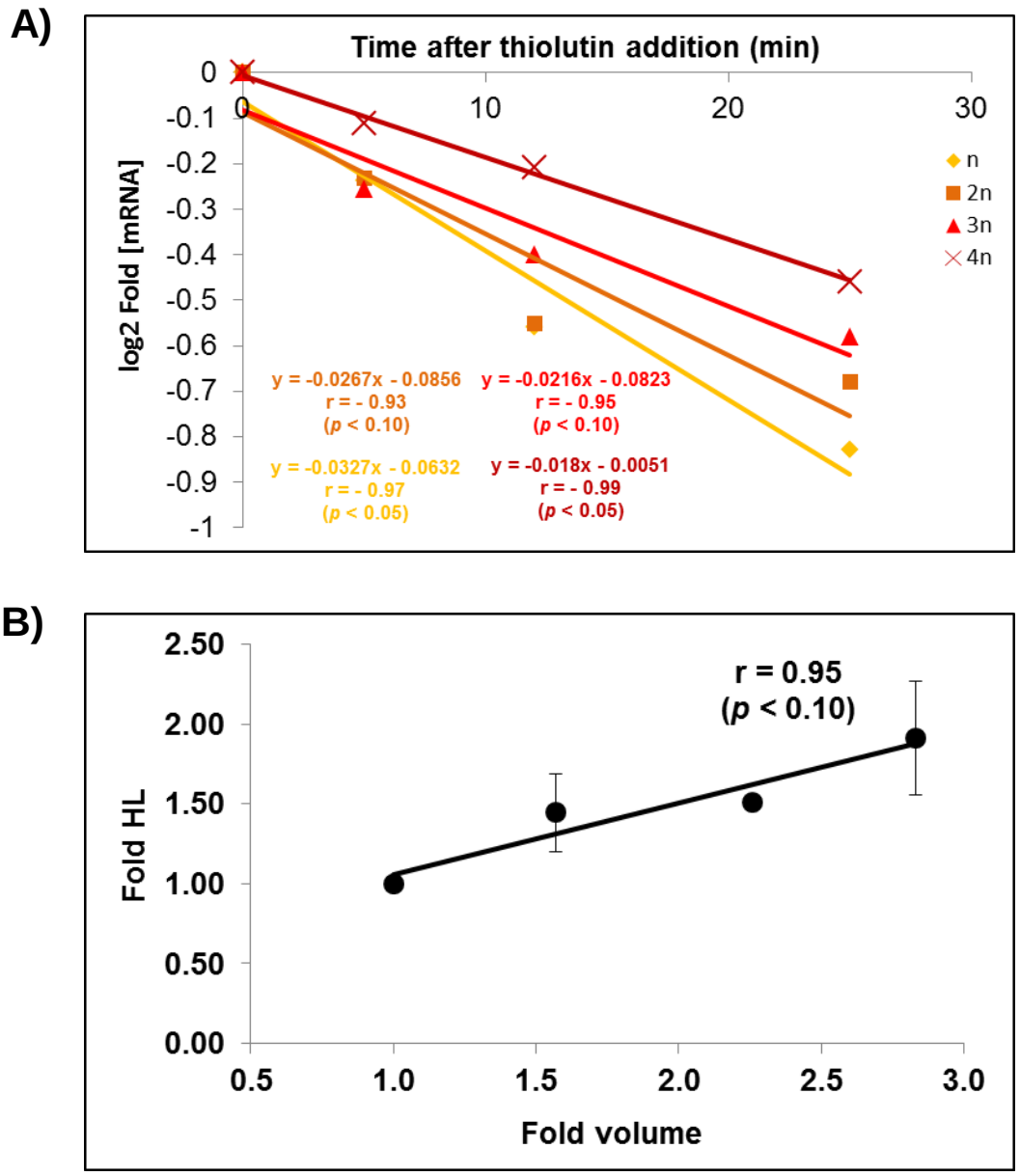

Figure S7. Global mRNA stability calculation by transcriptional shutoff with thiolutin in a series of polyploid strains. Cells were grown in rich media until the exponential phase. Immediately after taking the t0 sample, 5 µg/mL of thiolutin were added to the media and three additional time points were collected after shutoff (5, 12, and 25 min). A) Example of an experiment for global mRNA half-life (HL) determination in n-4n strains. B) Plot of the HL calculated from a series of 2-3 experiments identical to that shown in panel A showing the average value (fold with regard to haploid strain) and SD with regard to cell volume (see Figure S4C). Related to Figure 5.

A)

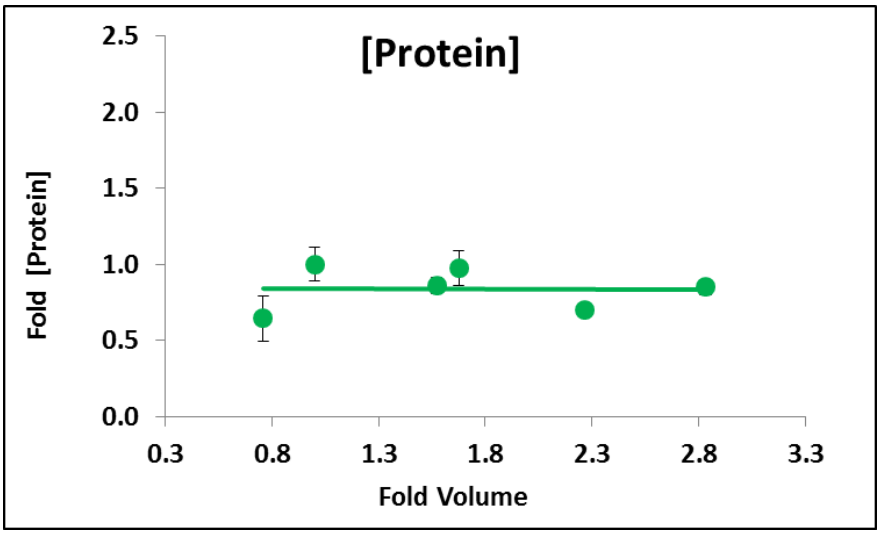

B)

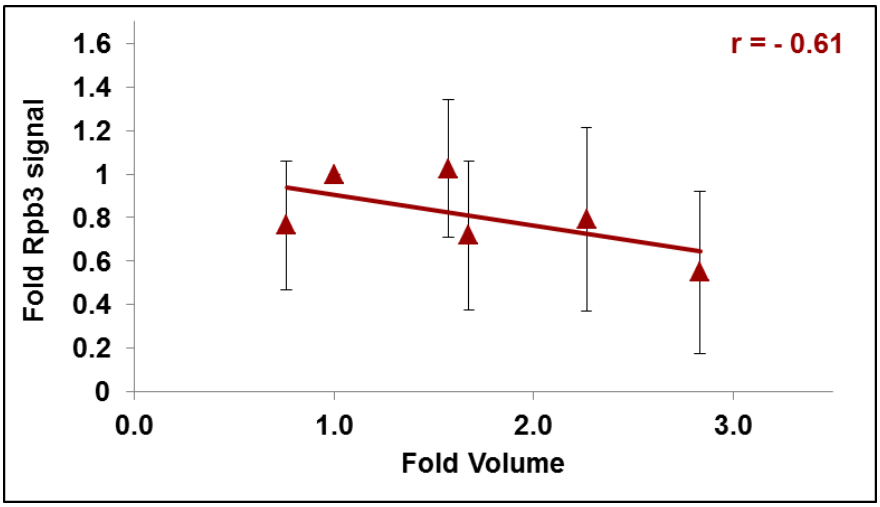

C)

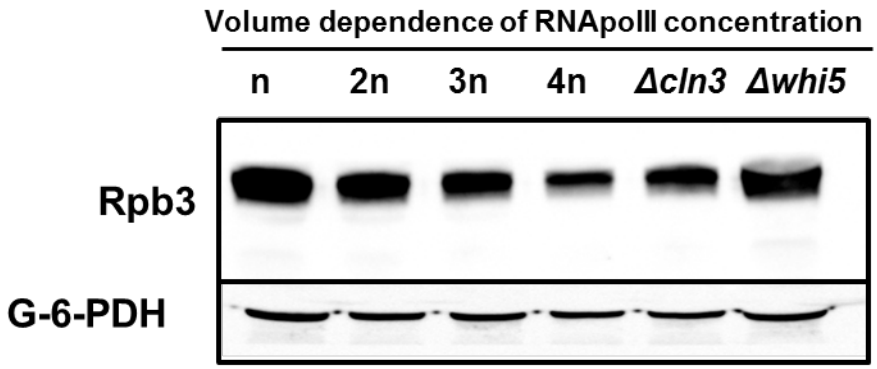

Figure S8. Western blot of RNA pol II in a series of polyploid and volume mutants. Total protein concentration is kept constant along the different strains. We show here (B) the results of an additional antibody (anti-Rpb3) to the ones shown in Figure 5. A representative example of the Western blots done with this antibody is shown (C). See Figure 5 for further details.

Appendix. Asymmetric cell division requires specific mechanisms for adjusting global transcription

Consider the following system of chemical reactions

$$RNAPol_{free} + DNA \xrightarrow{k_{on}} RNAPol_{bound},$$
$$RNAPol_{bound} \xrightarrow{k_{off}} RNAPol_{free} + DNA$$

The first two reaction represent binding/unbinding of a free RNA polymerase molecule to a DNA target site. We assume that the total number of RNA polymerase (free & bound) is given by R_cV, where V is cell volume, and R_c can be interpreted as RNA polymerase concentration. Furthermore, the total number of DNA targets is assumed to be M.

Let X and Y denote the number of free and bound RNA polymerase at equilibrium, respectively. Then, these variables satisfy the following constraints:

$$X + Y = R_cV \tag{1}$$
$$\frac{k_{on}}{V}(M - Y)X = k_{off}Y \tag{2}$$

Solving these equations gives the following number of bound RNA polymerase

$$Y = \frac{k_{on}M + k_{off}V + R_ck_{on}V - \sqrt{-4R_ck_{on}^2MV + (k_{off}V + k_{on}(M + R_cV))^2}}{2k_{on}}. \tag{3}$$

Next we try to simply the above expression. Note that (3) is a monotonically

increasing function with respect to size, with the following properties

$$Y \to 0 \quad \text{as} \quad V \to 0 \tag{4}$$

$$Y \to \frac{R_c k_{on} M}{k_{off} + R_c k_{on}} \quad \text{as} \quad V \to \infty. \tag{5}$$

Furthermore,

$$\frac{dY}{dV}|_{V=0} = R_c. \tag{6}$$

Assuming a Michaelis-Menten form for the function (3) with the exact same properties as in (4)-(6) yields

$$nTR := Y \approx \frac{R_c k_{on} MV}{k_{off} V + k_{on} M + k_{on} R_c V} \tag{7}$$

which essentially is the *nascent transcription rate (nTR).*

Scenario I: If RNA polymerase concentration R_c is small, and large number of DNA target M, then

$$nTR = \frac{R_c k_{on} MV}{k_{off} V + k_{on} M + k_{on} R_c V} \approx R_c V \tag{8}$$

and nTR becomes *size-dependent* and proportional to number of RNA polymerase.

Scenario II: If RNA polymerase concentration R_c is large, and low

number of DNA target M, then

$$nTR = \frac{R_c k_{on} MV}{k_{off} V + k_{on} M + k_{on} R_c V} \approx \frac{R_c k_{on} M}{k_{off} + k_{on} R_c} \tag{9}$$

and nTR becomes *size-independent* but dependent on the number of DNA targets.

Scenario III: In the above scenarios we have assumed that the total RNA polymerase concentration R_c is constant. Now consider an alternative assumption, where the total number of RNA polymerase molecules is constant (hence, concentration decreases with volume as seen in data). Assuming the system operates under scenario II, replacing R_c by R_n/V in Eq. 3

$$nTR \approx R_n \tag{10}$$

which is size-independent, and nTR per genome copy will decrease with increasing ploidy.